Progress In 3D Self-Consistent Full Wave-PIC Modelling Of Space Resolved ECR Plasma Properties

A. Pidatella[1], A. Galatà[2], G. S. Mauro[1], B. Mishra[1], E. Naselli[1], G. Torrisi[1], D. Mascali[1]

On behalf of the PANDORA collaboration

[1]Istituto Nazionale di Fisica Nucleare – Laboratori Nazionali del Sud – Catania (Italy)
[2]Istituto Nazionale di Fisica Nucleare – Laboratori Nazionali di Legnaro– Padova (Italy)

26th International Workshop on ECR Ion Sources
ECRIS24 - Darmstadt, Germany, September 15–19, 2024

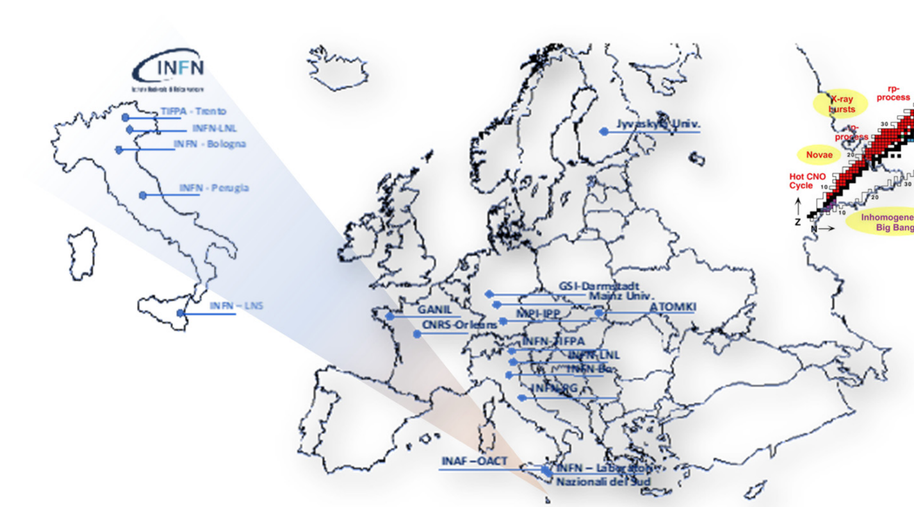

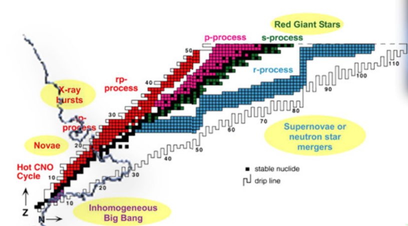

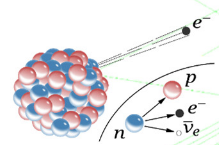

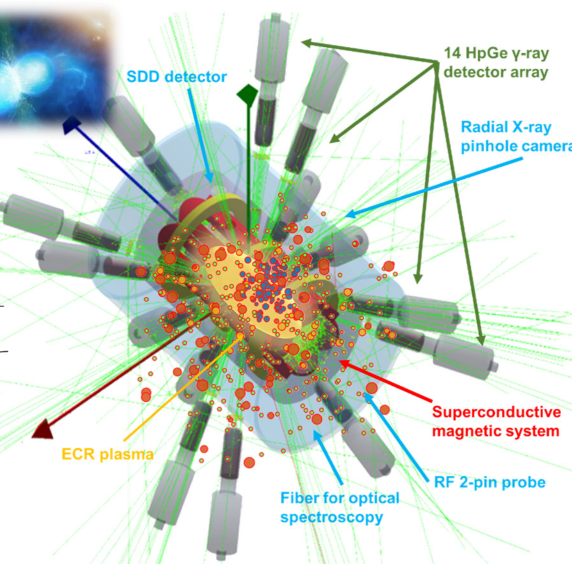

Plasmas for Astrophysics Nuclear Decay Observation and Radiation for Archaeometry

angelo.pidatella@lns.infn.it

Finanziato dall'Unione europea NextGenerationEU
Italiadomani
NQSTI National Quantum Science and Technology Institute

ECR plasma modelling – WHY?

ECR plasmas generated in ECR Ion Sources or Trap can be used to carry out fundamental research and to improve particle accelerators' performances

Models consistently describing the **plasma generation**/sustainment and the **particle/radiation interactions in plasma** are needed to constrain the ECR plasma physics and all processes occurring inside it

ECR plasmas properties are **non-uniform**, strongly **inhomogeneous and anisotropic**

SPECIFICALLY FOR ECRIS models can:

- *Improve fundamental undertanding of ECRIS devices*
- *Couple with diagnostics for extracting plasma parameters and observables*
- *Investigating on plasma turbulences to mitigate ECRIS instabilities*

BUT MORE IN GENERAL models can:

- Serve to multi-physics and multi-disciplinary experiments to complement the physics description
- Connecting laboratory ECR plasma theory and experiments…**let's give an example**…

PANDORA: an ECR Trap for Nuclear Astrophysics and Multi-Messenger Astronomy

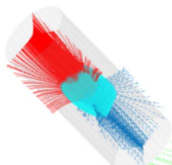

Microwaves igniting and sustaining plasma, 5 kW and 18-21 GHz

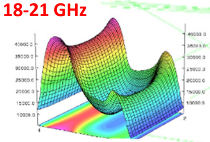

See talk *by* G. Mauro

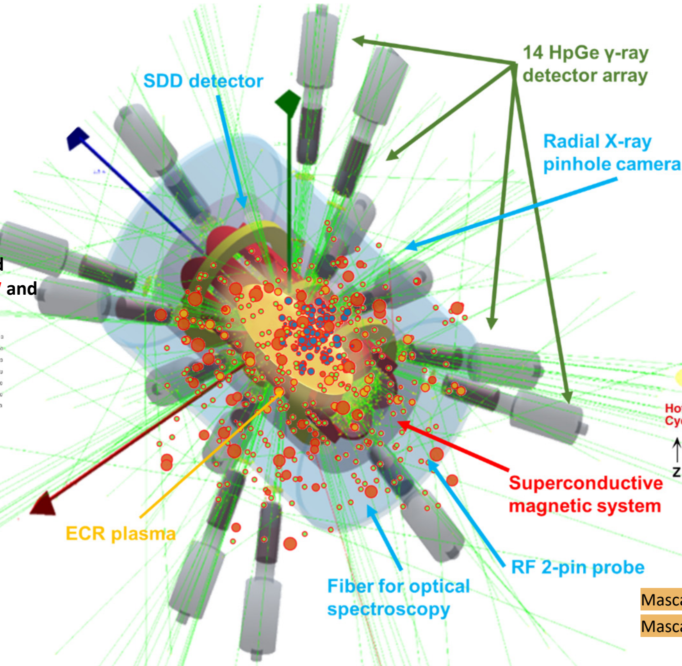

Busso, M. *et al.*, Ann Rev Astron. Astrophys. **37** (1999) 239
Cristallo, S. *et al.*, APJ Suppl. **197**, 17 (2011)
Palmerini, S. *et al* (2021) APJ **921** 7

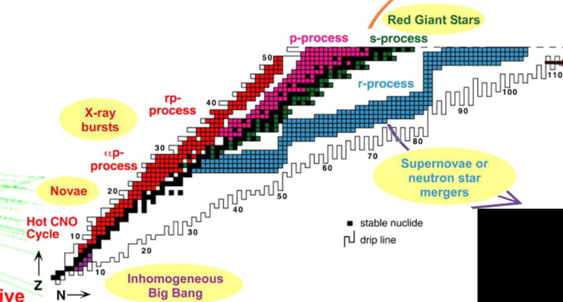

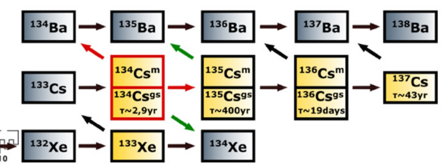

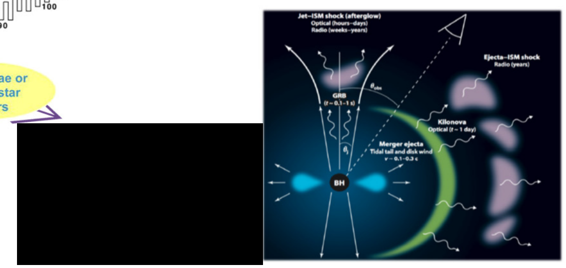

Metzger B.D., Kilonovae. Living Rev Relativ 23, 1 (2020)

Mascali D., *et al*, Eur. Phys. J. A (2017) 53: 145
Mascali D., *et al*, Universe 8 (2), 80 (2022)

PANDORA (*Plasmas for Astrophysics Nuclear Decays Observation and Radiation for Archaeometry*) **plasma trap** for inter-disciplinary studies: **atomic physics**, **astrophysics,** and **nuclear astrophysics**

1. **Nuclear bound-β decay rate** in a high-energy content plasma for nuclei relevant in *s*-process branching
   Pidatella, A. *et al.,* Plasma Phys. Control. Fusion **66** (3), 035016 (2024)
   Mishra, B., *et al*., Front. in Physics, **10**, 932448, (2022)
   Galatà, A., *et al*., Front. in Physics, **10**, 947194, (2022)
2. **Magneto-plasma opacity spectroscopic measurements** relevant for KN light-curve and *r*-process nucleosynthesis yields
   Pidatella, A., et al. Nuovo Cimento 44 C (2021) 65
   Pidatella, A., *et al.* Frontiers in Astronomy and Space Sciences, 10.3389/fspas.2022.931744 (2022)
3. **Plasma kinetic turbulences** and impact on astrophysics
   Mascali D., *et al* (2022) *Plasma Phys. Control. Fusion* **64** 035020

See talk *by* D. Mascali

ECR plasma modelling – HOW?

Outline:

Multiphysics Simulations, Theory and Modelling for ECRIS and for PANDORA

- **Plasma kinetics:** stationary PIC-Particle-In-Cell simulation by Relativistic Boris Leap-Frog Method implemented in MATLAB
- **Plasma Collisions & Reactions:** Monte-Carlo approach embedded in the PIC-code
- **Electromagnetic interaction with plasma:** self-consistent evaluation of the field by FEM code with tensorial computation (COMSOL)

Specific interest for PANDORA

- **Nuclear decay rate evaluation:** generalization of the Fermi-Golden Rule to LTE and NLTE multi-ionized media (laboratory and astrophysical plasmas)
- **Gamma-ray detection simulation:** GEANT4 simulation including the plasma source, magnets, cryostat and HPGe detectors array to perform detection efficiency calculations and virtual experiments
- **Radioactive isotope injection:** evaporation dynamics and coupling to the plasma of metallic isotope

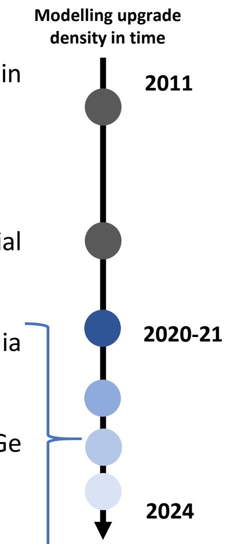

Simulations and results presented will refer to different ECR Ion Sources/Trap scenarios:

- **ATOMKI, Debrecen (HU) ECRIS:** 12.84 GHz, 200 W, B-min, $L_{ECR}*R^2_{ECR} \sim 11\ cm^3$
- **INFN-LNL, Legnaro (IT) ECRIS – LEGIS:** 14.428 GHz, 100 W, B-min, $L_{ECR}*R^2_{ECR} \sim 7\ cm^3$
- **INFN-LNS, Catania (IT) ECRIT – PANDORA:** 18 GHz, 5 kW, B-min, $L_{ECR}*R^2_{ECR} \sim 1400\ cm^3$

	VENUS	ASTERICS	unit
L	500	600	mm
R	72	91	mm
V	8.1	15.6	liters
B_{wall}	1.85	1.97	T
L_{ECR}	178	205	mm
R_{ECR}	50	58	mm

T. Thuillier et al 2024 J. Phys.: Conf. Ser. 2743 012059

ECR plasma modelling – pipeline

In ECR magnetoplasma, **electrons interact strongly with microwave radiation** so **full-wave PIC electron kinetics models** are required. The plasma is NLTE so **ion kinetics is studied using PIC-MC simulations that can solve Collisional-Radiative model**

PIC SIMULATIONS FOR ELECTRONS

3D, steady-state maps of n_e and E_e

First level input to all codes and therefore precision needed

Observables: **Soft X-ray spectroscopy**, interferometry, polarimetry

PIC-MC SIMULATIONS FOR PLASMA IONS

3D, steady-state maps of <*Z*> and n_i

Second level input to in-plasma decay code

Observables: **Faraday cup (CSD)**, optical emission spectroscopy, X-ray fluorescence

Specific interest for PANDORA

PIC-MC SIMULATIONS FOR ISOTOPE IONS

3D, steady-state maps of <*Z*> and λ^*

Observables: **PANDORA**

Plasma Electron Simulations - Overview

PIC simulation for ECR plasma electrons
- Description: Vlasov-Maxwell equation
- Scaling: Plasma cutoff density
- Self-consistency: Microwave EM field (GHz)

D. Mascali, et al , Eur. Phys. J. D. **69**, 27 (2015)
A. Galatà *et al*, Front. Phys. **10**, 947194 (2022)
B. Mishra *et al*, Front. Phys. **10**, 932448 (2022)

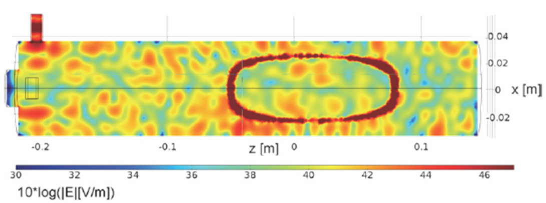

Example of mode-like EM field structure in plasma as self-consistently arising from simulations

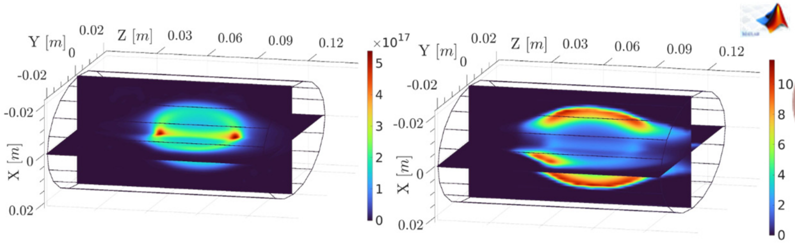

Electron density n_e (m^{-3}) and mean energy E_e (keV) maps for the LEGIS source (INFN-LNL) obtained from PIC simulations.

Schematic of COMSOL Multiphysics© + MATLAB© self-consistent numerical modelling for electrons

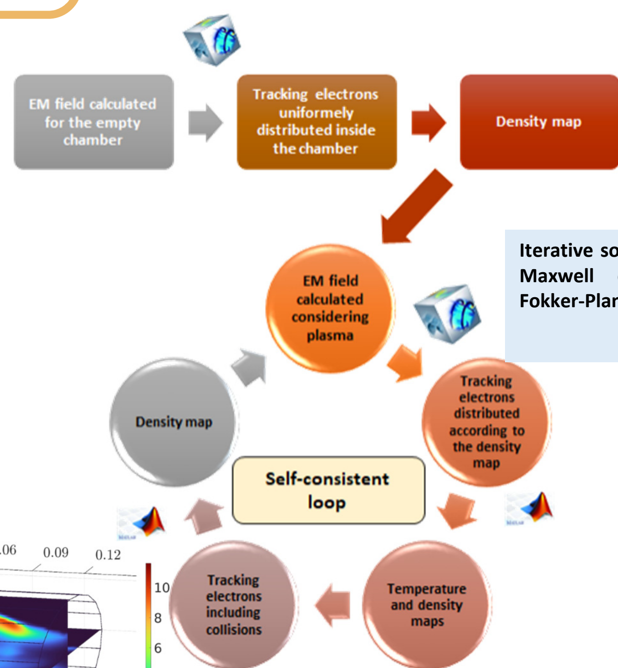

Iterative solution of Vlasov-Maxwell equations with Fokker-Planck collisions

Vlasov-Maxwell equation (*cold approximation*)

$$\frac{\partial f_\alpha}{\partial t} + \boldsymbol{v}\cdot\frac{\partial f_\alpha}{\partial \boldsymbol{r}} + \frac{q_\alpha}{m_\alpha}(\boldsymbol{E}+\boldsymbol{v}\times\boldsymbol{B})\cdot\frac{\partial f_\alpha}{\partial \boldsymbol{v}} = 0$$

Collisional term (collective) solving the Fokker-Planck equation

$$\mathscr{D} f = \mathbb{C} = -\frac{\partial}{\partial \mathbf{v}}\cdot(\mathbf{A}f) + \frac{1}{2}\frac{\partial^2}{\partial\mathbf{v}\partial\mathbf{v}} : (\mathbf{B}f)$$

BORIS METHOD

Set of equations for transporting particles under Lorentz force

↓

LANGEVIN EQUATION

Formalism for including diffusion and friction forces for velocity evolution

Self-consistent, steady-state solution

Plasma Electron Simulations - Overview

Maxwell's eqs.

$$\vec{\nabla}\times\vec{E}(\vec{r}) = -i\omega\vec{B}(\vec{r})$$
$$\vec{\nabla}\times\vec{H}(\vec{r}) = i\omega\varepsilon_0\vec{E}(\vec{r}) + \vec{J}(\vec{r}) = i\omega\overline{\overline{\varepsilon}}\cdot\vec{E}(\vec{r}) = i\omega\cdot\vec{D}(\vec{r})$$
$$\vec{\nabla}\cdot\vec{D}(\vec{r}) = \rho(\vec{r})$$
$$\vec{\nabla}\cdot\vec{B}(\vec{r}) = 0$$

Constitutive relations

$$\vec{J} = \overline{\overline{\sigma}}\cdot\vec{E}$$
$$\vec{D} = \frac{\vec{J}}{i\omega} + \varepsilon_0\vec{E} = \left(\frac{\overline{\overline{\sigma}}}{i\omega} + \varepsilon_0\right)\vec{E} = \overline{\overline{\varepsilon}}\cdot\vec{E}$$
$$\overline{\overline{\varepsilon}} = \varepsilon_0\left(\overline{\overline{I}} - i\frac{\overline{\overline{\sigma}}}{\omega\varepsilon_0}\right)$$

Non-uniform *local* dielectric tensor

$$= \epsilon_0 \begin{bmatrix} 1 + i\frac{\omega_p^2}{\omega}\frac{a_x}{\Delta} & i\frac{\omega_p^2}{\omega}\frac{c_z + d_{xy}}{\Delta} & i\frac{\omega_p^2}{\omega}\frac{-c_y + d_{xz}}{\Delta} \\ i\frac{\omega_p^2}{\omega}\frac{-c_z + d_{xy}}{\Delta} & 1 + \frac{i\omega_p^2}{\omega}\frac{a_y}{\Delta} & i\frac{\omega_p^2}{\omega}\frac{c_x + d_{yz}}{\Delta} \\ i\frac{\omega_p^2}{\omega}\frac{c_y + d_{xz}}{\Delta} & i\frac{\omega_p^2}{\omega}\frac{-c_x + d_{zy}}{\Delta} & 1 + i\frac{\omega_p^2}{\omega}\frac{a_z}{\Delta} \end{bmatrix}$$

3D *Cold* plasma modelling: dispersive medium with collisions

Random thermal motion neglected
($v_\varphi >> v_{th}$)

$$m\frac{\partial\vec{v}}{\partial t} = \left(q\vec{E} + \vec{v}\times\vec{B}_0\right) - \omega_{eff} m\vec{v}$$

COLLISION FREQUENCY ω_{eff} ACCOUNTS FOR THE **COLLISION FRICTION**, MODELS THE **WAVE DAMPING** AND RESOLVES THE **SINGULARITY** OF SOME ELEMENTS OF TENSOR

SOLUTION OF WAVE EQUATION WITH ADAPTIVE MESH IN FEM SOLVER

- Non-homogeneous dielectric permittivity tensor depends on local electron density and magnetic field

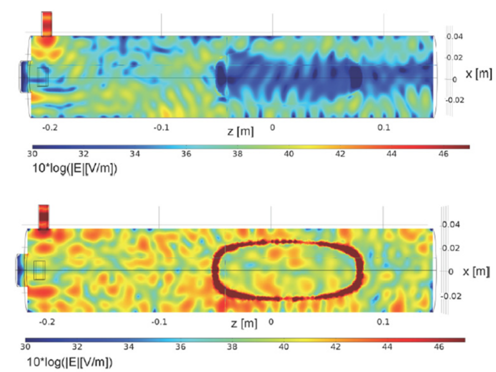

Uniform (top) vs. *non-uniform tensor* (bottom) wave-to-plasma coupling

Plasma Electron Simulations - Overview

Particle Transport

Being charged particles, ions in an ECR plasma move under the influence of EM fields (self-generated and external) and undergo Coulomb collisions with other plasma species

EM transport

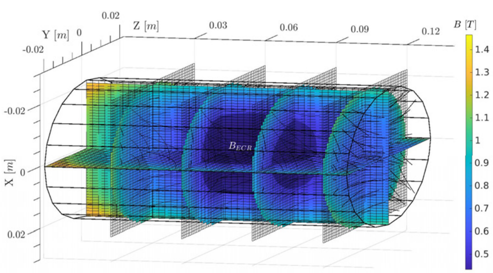

Magnetostatic field profile in the LEGIS

$$\frac{d\mathbf{r}}{dt} = \mathbf{v}$$
$$m\frac{d\mathbf{v}}{dt} = q(\mathbf{E} + \mathbf{v}\times\mathbf{B})$$

Equation of motion for charged particles under Lorentz force

$$\frac{\mathbf{r}^{n+1} - \mathbf{r}^{n}}{T_{step}} = \mathbf{v}^{n+1/2}$$
$$\mathbf{u}^{-} = \gamma\mathbf{v}^{n+1/2} + \frac{q}{2m}\mathbf{E}^{n+1}T_{step}$$
$$\theta = \frac{qT_{step}}{m\gamma}|\mathbf{B}^{n+1}|$$
$$\mathbf{t} = \tan\frac{\theta}{2}\mathbf{b}$$
$$\mathbf{u}^{'} = \mathbf{u}^{-} + \mathbf{u}^{-}\times\mathbf{t}$$
$$\mathbf{u}^{+} = \mathbf{u}^{-} + \frac{1}{2+|\mathbf{t}|^2}(\mathbf{u}^{'}\times\mathbf{t})$$
$$\mathbf{v}^{n+3/2} = \frac{1}{\gamma}(\mathbf{u}^{+} + \frac{q}{2m}\mathbf{E}^{n+1}T_{step})$$

Numerical implementation of Lorentz force using Boris method, with correction by Zenitani and Umeda

$$\mathbf{u}^{+} = R_{rot}\mathbf{u}^{-}$$

J.P. Boris, Proc. 4th Naval Conf. on Numerical Simulation of Plasmas
S. Zenitani and T. Umeda, Phys. Plasmas **25** (2018)

Collisions

Numerical implementation of Fokker-Planck equation using superpotential formalism by MacDonald and Rosenbluth

W.M. MacDonald, M.N. Rosenluth and W. Chuck, Phys. Plasmas **107**, 350 (1957)
A. Galatà et al, Plasma Sources Sci. Technol. **25** (2016)

$$D_{||} = \langle \mathbf{v}_{||}^2 \rangle = \frac{A_D}{|\mathbf{v}^{n+1/2}|}G(\frac{|\mathbf{v}^{n+1/2}|}{c_s})$$
$$A_D = \frac{(ZZ')^2 e^4 n_s \ln\Lambda}{2\pi\epsilon_0^2 m^2}$$
$$D_{\perp} = \langle \mathbf{v}_{\perp}^2 \rangle = \frac{A_D}{|\mathbf{v}^{n+1/2}|}\left\{\Phi(\frac{|\mathbf{v}^{n+1/2}|}{c_s}) - G(\frac{|\mathbf{v}^{n+1/2}|}{c_s})\right\}$$
$$\nu_s = \left(1 + \frac{m}{m_s}\right)\frac{A_D}{c_s^3}\frac{G(\frac{|\mathbf{v}^{n+1/2}|}{c_s})}{\frac{|\mathbf{v}^{n+1/2}|}{c_s}}$$
$$\mathbf{v}_{fric} = \nu_s\mathbf{v}^{n+1/2}T_{step}$$
$$\mathbf{v}_{rand} = P_{||}N(0, D_{||}) + P_{\perp}N(0, D_{\perp})$$

$$\mathbf{v}^{n+3/2} = \frac{1}{\gamma}(\mathbf{u}^{+} + \frac{q}{2m}\mathbf{E}^{n+1}T_{step}) + \mathbf{v}_{fric} + \mathbf{v}_{rand}$$

Plasma Ion Simulations - Overview

PIC simulations for ECR plasma ions:
- Description: Steady state electron maps + *Balance equation*
- Scaling: Quasi-neutrality with electron density
- Self-consistency: Electron density and energy maps

B. Mishra *et al*, Front. Phys. **10**, 932448 (2022)
B. Mishra, EPJ WoC **275**, 02001 (2023)

3 core modules

Ion Transport

Transport in EM fields under Lorentz force

Poisson solver for ES field due to local charge unbalance

Collisions by Fokker-Planck equation

MC Sampling

$$\frac{\mathrm{d}n_i}{\mathrm{d}t} = \boxed{n_{i-1}n_e\gamma_{i-1,i} - n_i n_e \gamma_{i,i+1}} + \boxed{n_{i+1}n_0 E_{i+1,i} - n_i n_0 E_{i,i-1}} - \frac{n_i}{\tau_i}$$

Electron impact ionization (EI)
Ion impact charge exchange (CEX)

Density Scaling

Iterative scaling of ion occupation map

$$\int_V n_e \mathrm{d}V = K \int_V w_i n_i$$

Plasma Ion Simulations - Modules

ECR plasma ions can be simulated PIC-MC codes, which evolve the density maps of successive ionization stages self-consistently with electron density and energy maps given as input

B. Mishra et al, Front. Phys. **10**, 932448 (2022)
B. Mishra, EPJ WoC **275**, 02001 (2023)

BUFFER IONS BALANCE EQUATION:

$$\frac{\mathrm{d}n_i}{\mathrm{d}t} = n_{i-1} n_e \gamma_{i-1,i} - n_i n_e \gamma_{i,i+1} + n_{i+1} n_0 E_{i+1,i} - n_i n_0 E_{i,i-1} - \frac{n_i}{\tau_i}$$

KEYWORD(S): Steady state

The contribution from each process can be evaluated independently to construct CSD

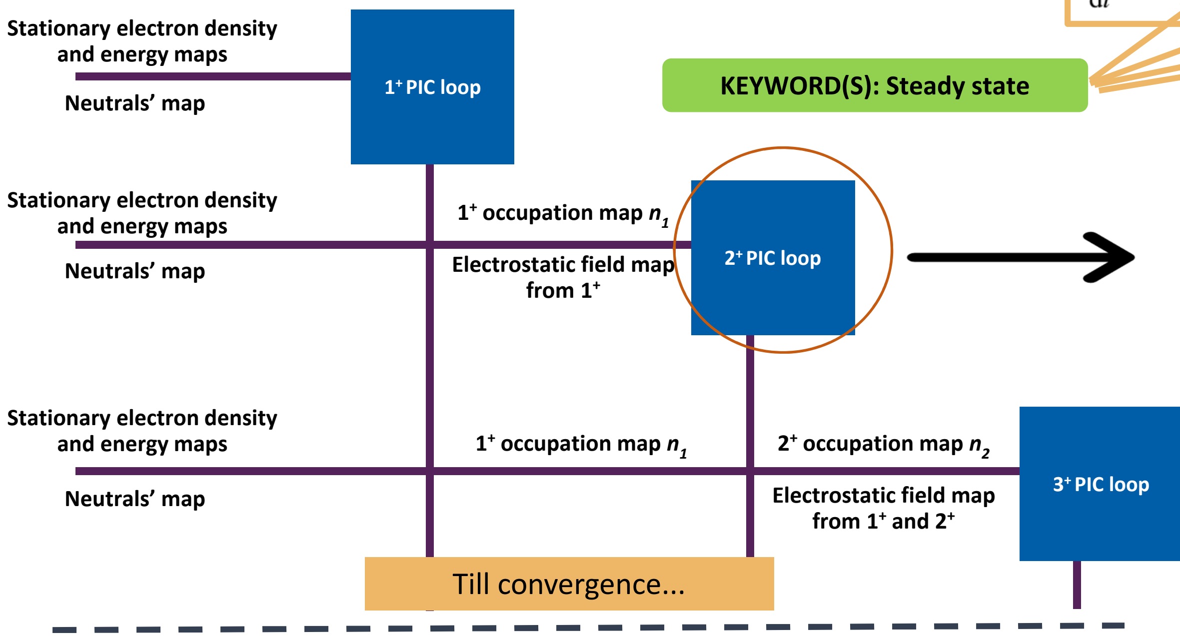

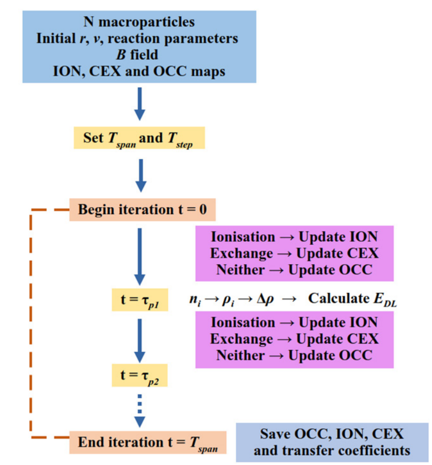

Plasma Ion Simulations - Modules

MC Sampling

Ions in a plasma can interact with each other and electrons to undergo competing reactions.

Ion transport occurs simultaneously with reactions, which can be sampled using MC methods

$$\frac{dn_i}{dt} = \boxed{n_{i-1}n_e\gamma_{i-1,i} - n_i n_e \gamma_{i,i+1}} + \boxed{n_{i+1}n_0 E_{i+1,i} - n_i n_0 E_{i,i-1}} - \frac{n_i}{\tau_i}$$

<u>**Electron impact ionization (EI)**</u>

<u>**Ion impact charge exchange (CEX)**</u>

$$\nu_{ion} = n_e \sigma_{ion,i\rightarrow i+1} v_{e,rel}$$

$$\nu_{CEX} = n_0 \sigma_{CEX,i\rightarrow i-1} v_{i,rel}$$

$$\sigma_{ion,i\rightarrow i+1} = \frac{10^{-17}}{I_i E_e}\left[\sum_{n=1}^{6} A_n \left(1-\frac{I_i}{E_e}\right)^n + B\ln\left(\frac{E_e}{I_i}\right)\right]$$

Lotz, W., Zeitschrift fur Physik 216, pp. 241–247, (1968).

$$\sigma_{CEX,i\rightarrow i-1} = A i^{\alpha}(I_0)^{\beta}$$

Müller, A. *et al.*, Phys. Lett. A, 62A:391-4, (1977).

ECRIS	ω	P_{inj}	Gas	P	r	L
A-LPC	12.84 GHz	30 W	Ar	10^{-6} mbar	29 mm	210 mm
A-HPC	14.25 GHz	200 W	Ar	10^{-6} mbar	29 mm	210 mm
LEGIS	14.428 GHz	100 W	O	5×10^{-5} mbar	25 mm	130 mm

The plots comparing *volume-averaged (on n_e and E_e)* frequencies of EI and CEX processes offer insight into the dynamics of atomic processes as a function of ionisation stage.

$$\begin{aligned} P_{tot}(T_{step}) &= 1 - e^{-\nu_{tot}T_{step}} = \frac{\nu_{ion}+\nu_{CEX}}{\nu_{tot}}(1-e^{-\nu_{tot}T_{step}}) \\ &= \frac{\nu_{ion}}{\nu_{tot}}(1-e^{-\nu_{tot}T_{step}}) + \frac{\nu_{CEX}}{\nu_{tot}}(1-e^{-\nu_{tot}T_{step}}) \\ &= P_{ion}(T_{step}) + P_{CEX}(T_{step}) \end{aligned}$$

- Ionisation if $0 <= r < P_{ion}$
- CEX if $P_{ion} <= r < (P_{ion} + P_{CEX})$
- Nothing if $(P_{ion} + P_{CEX}) <= r < 1$

- CEX and EI depend on ECRIS tuning parameter: **pressure, power, species, CSD**
- Modelling processes can **help in experimentally fine-tuning the CSD**

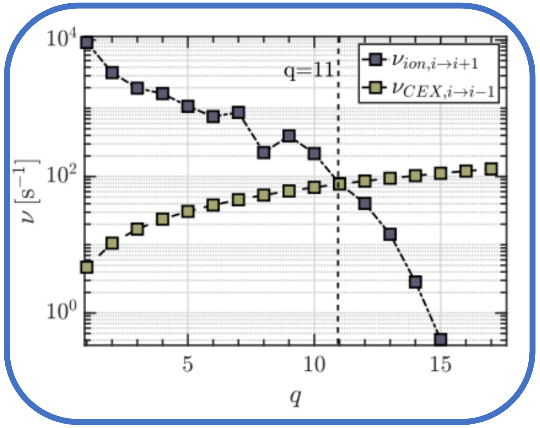

Comparison between averaged EI and CEX frequencies in ATOMKI ECRIS with argon (top) and LEGIS with oxygen (bottom)

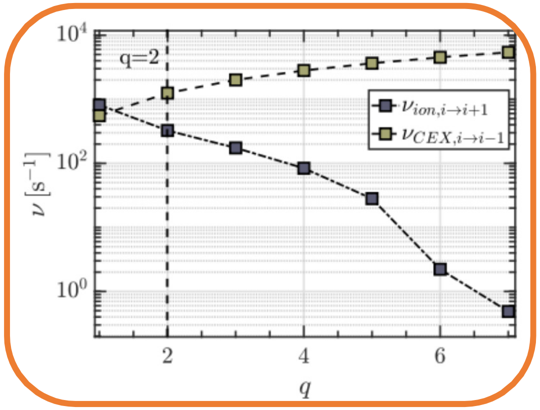

Plasma Ion Simulations - Modules

Density Scaling and CSD

The results of ion transport + MC sampling are 3D accumulation maps which denote relative particle occupation in each simulation cell, and **transfer coefficient** which **weigh the accumulation maps** according to EI and CEX reactions.

The accumulation maps can be **scaled by considering global charge neutrality with electrons**

Example: After simulating first 3 charge states…

$$\begin{aligned}\oint_V n_e \mathrm{d}V = \boxed{K_3}\Big[&(1-\boxed{k_{1\to2}}+2k_{1\to2}k_{2\to1}+k_{1\to2}k_{2\to3}k_{3\to2})\oint_V N_1\mathrm{d}V+\\ &2k_{1\to2}(1-k_{2\to3}-k_{2\to1}+k_{2\to3}k_{3\to2})\oint_V N_2\mathrm{d}V+\\ &3k_{1\to2}k_{2\to3}(1-\boxed{k_{3\to4}}-k_{3\to2})\oint_V N_3\mathrm{d}V+\\ &4k_{1\to2}k_{2\to3}k_{3\to4}\oint_V N_{3\to4}\mathrm{d}V\Big]\end{aligned}$$

Transfer coefficients

Scaling coefficient

$$n_1 = K_3(1-k_{1\to2}+2k_{1\to2}k_{2\to1}+k_{1\to2}k_{2\to3}k_{3\to2})n_1$$
$$n_2 = K_3k_{1\to2}(1-k_{2\to3}-k_{2\to1}+k_{2\to3}k_{3\to2})n_2$$
$$n_3 = K_3k_{1\to2}k_{2\to3}(1-k_{3\to4}-k_{3\to2})n_3$$

Scaling the density also helps evaluating self-consistently the electrostatic double layer field

*D. Mascali et al, Rev. Sci. Instrum. **83** (2012)*
*K. Takahashi, T. Kaneko and R. Hatakeyama, Phys. Plasmas **15** (2008)*

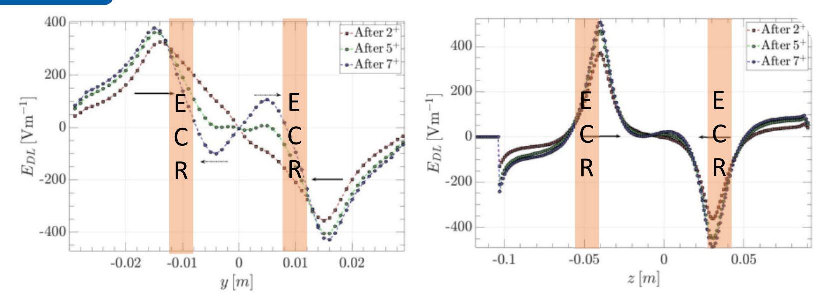

Iterative evolution of the double layer electrostatic field arising self-consistently with charge separation in the plasma, along *y*- and *z*-axes

Plasma Electron Simulations – Exp. benchmark

Plasma **diagnostic technique** developed by INFN – LNS, Catania and ATOMKI, Debrecen to study properties of warm/hot electrons in ECR plasma using **volumetric and space-resolved soft X-ray spectroscopy** (2 < $E_{h\nu}$ < 30 keV)

*R. Racz, D. Mascali et al , Plasma Sources Sci. Technol. **26**, 075011 (2017)*
*D. Mascali et al, Rev. Sci. Instrum. **87**, 02A510 (2016)*

Raw data from SDD detector can be converted into X-ray emissivity density by calibration with Fe lines and correction for quantum efficiency and dead time

B. Mishra et al , Phys. Plasmas. 28, 102509 (2021)
B. Mishra et al, Cond. Matter (2021)

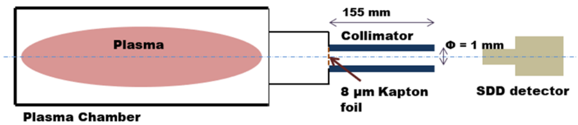

Volumetric X-ray emission from near-axis region, measured using SDD detector + collimator

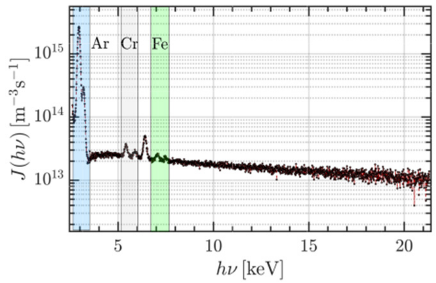

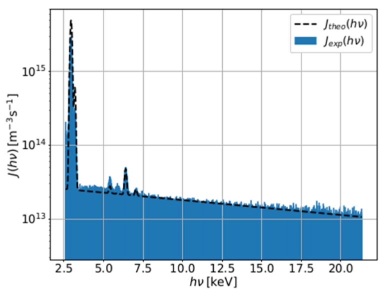

X-Ray Emissivity Model

$$J_{theo,brem}(h\nu) = n_e n_i (Z\hbar)^2 \left(\frac{4\alpha}{\sqrt{6m_e}}\right)^3 \sqrt{\frac{\pi}{k_B T_e}} e^{-h\nu/k_B T_e}$$

$$J_{nl\to nl'} = \frac{h\nu_{nl\to nl'}}{\Delta E} n_e n_i \omega_{nl\to nl'} \int_I^\infty \sigma_{nl,ion}(E) v_e(E) f(E) \mathrm{d}E$$

See talk *by* E. Naselli

Extracting warm electron parameters from different plasma zones generates observables against which the PIC simulation results can be benchmarked

Space-resolved energy density + K-Shell ionisation cross-section + Local geometrical efficiency

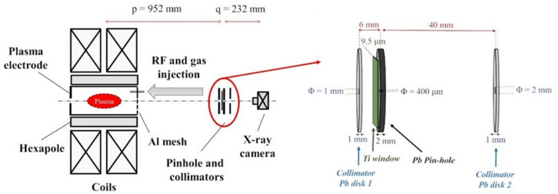

*E. Naselli et al, Condens. Matter **7**, 1 (2022)*
G. Finocchiaro et al, Phys. Plasmas 31, 6 (2024)

Space-resolved X-ray emission from different plasma zones, measured using CCD camera + pinhole

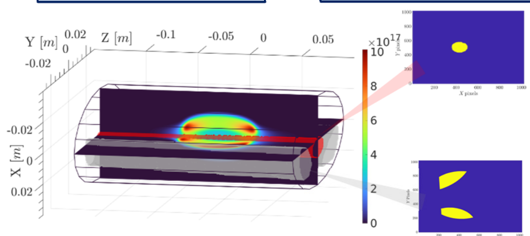

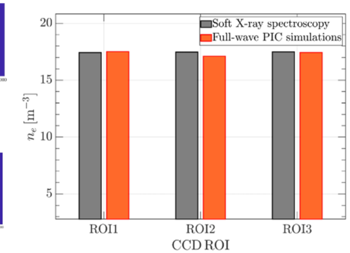

Plasma Ion Simulations – Results and exp. benchmark

The main results of the PIC-MC simulations are 3D steady-state maps of ion density in for each ionisation stage and <*Z*>

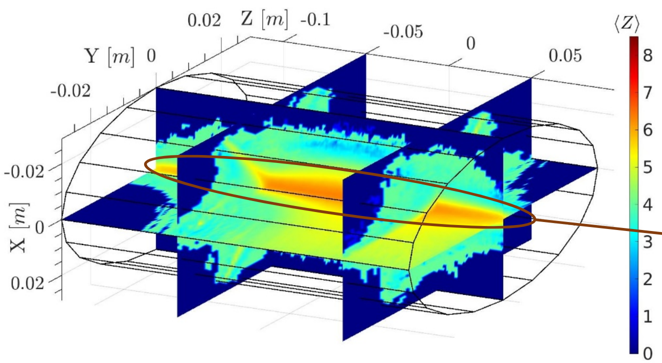

<Z> of Ar plasma in ATOMKI ECRIS from PIC-MC code (*top*) and of Oxygen plasma in LNL LEGIS (*bottom*)

- Higher charge states accumulate in the near-axis: due to their generation from lower charge states through EI in regions with high E_e, and strongly confined by E_{DL} and diffusion

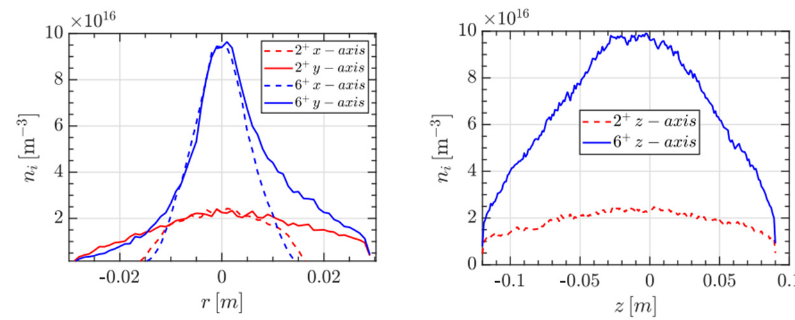

n_i of Ar^{2+} and Ar^{6+} in ATOMKI ECRIS along the radius and axis in (*top*) and same for O^{1+} and O^{3+} in LEGIS (*bottom*)

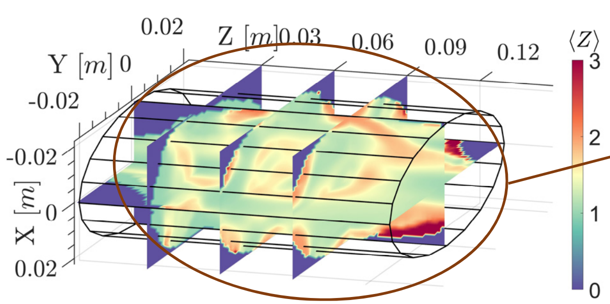

- Results may vary according to the geometry of the system, the magnetostatic field and type of ions (which govern particle transport), and steady state n_e, k_BT_e maps

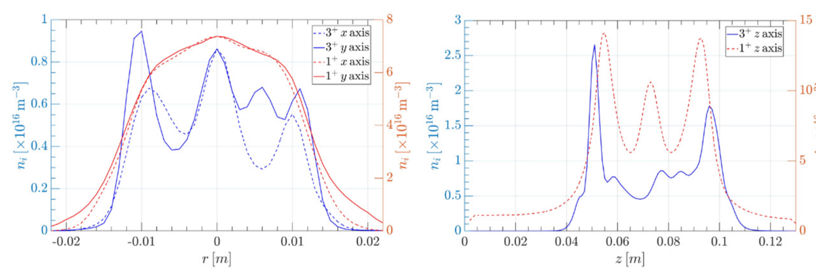

Plasma Ion Simulations – Results and exp. benchmark

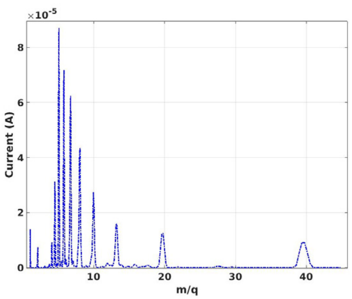

Experimental spectrum of Ar ion current [**]

L = 105 mm
Φ_{ext} = 11 mm
$\langle N_i \rangle$ = Mean density in region of potential dip

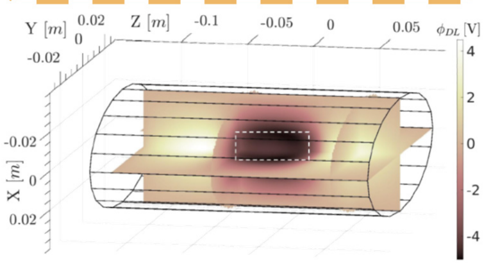

$$I_i = \kappa \frac{(2L)S}{2} \frac{\langle N_i \rangle q_i e}{\tau_i}$$

$$\tau_{ES,i} = R \frac{\sqrt{\pi} L}{v_i} \exp\left(\frac{q_i e \langle \phi_{DL} \rangle}{k_B T_i} \right)$$

$$\tau_{d,i} = 7.1 \times 10^{-20} L q_i \ln \Lambda \sqrt{A} \, \frac{n_e Z_{eff}}{k_B T_i^{3/2} E}$$

$$\frac{1}{\tau_i} = \boxed{\frac{1}{\tau_{ES,i}} + \boxed{\frac{1}{\tau_{d,i}}}}$$

- The **double layer confinement** plays a fundamental role in reproducing the experimental CSD of extracted ion beam
- Predicting **how much intense** and **where the CS distributes** in the ECRIS could help in **optimizing** it for a **desired beam**

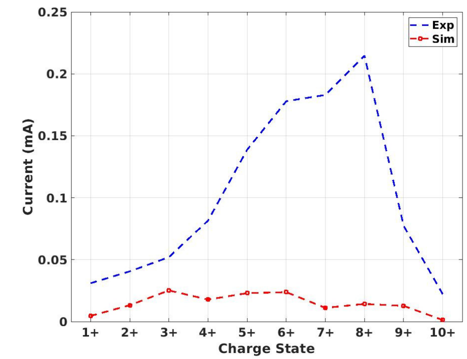

Simulated spectrum of Ar ion current with ambipolar diffusion alone

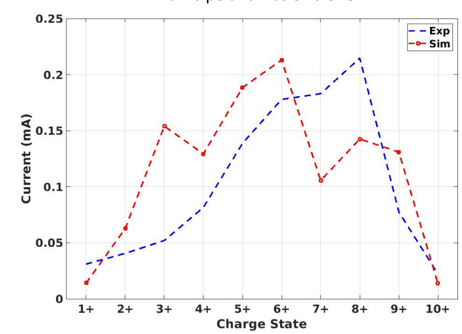

Simulated spectrum of Ar ion current with ambipolar diffusion and double layer confinement

B. Mishra *et al*, Frontiers in Physics 10:932448
[**] S. Biri *et al*, Rev. Sci. Instrum. 83, 02A431 (2012)

APPLICATIONS & RESULTS

APPLICATION - Study of metal evaporation dynamics in ECRIS

Pidatella, A. *et al.*, Plasma Phys. Control. Fusion **66** (3), 035016 (2024)

WHY?

- **PANDORA focus**: poisoning of γ-ray signal-to-background ratio at HpGe detection array from decaying **^{134}Cs** neutrals deposited on chamber wall

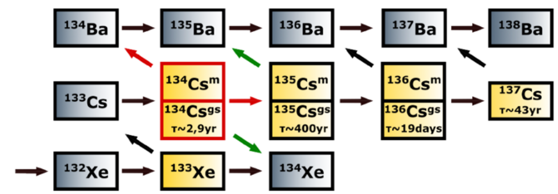

- **Injection via resistively heated ovens** for **Cs (~420 K)** - 1 ppm w.r.t. plasma ion density

Isotope	$t_{1/2}$ [yr]	E_γ [keV]
^{176}Lu	$3.78 \cdot 10^{10}$	202.88 & 306.78
^{134}Cs	**2.06**	**795.86**
^{94}Nb	$2.03 \cdot 10^{4}$	871.09

- ***Expected measurement time for ^{134}Cs: 12 h***
- ***Expected quantity used: 5.5E-10 mg of ^{134}Cs***

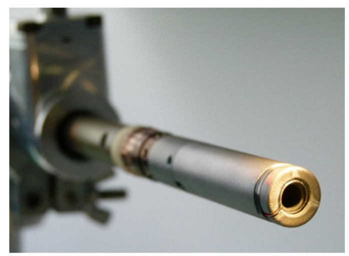

Courtesy of F. Maimone and GSI colleagues

Study of metallic atoms diffusion, transport, and deposition in ECR plasma evidencing the plasma role on a space-dependent ionisation

HOW?

- **Monte Carlo particle mover: time-dependent** thermal diffusion (atoms), reaction (ionised), transport of ions ($q=1^+$), and deposition according to **ECR plasma dynamics model**

- **Reaction maps: self-consistent Particle-In-Cell PANDORA plasma simulation** (EM field coupled to particle motion in trap) providing 3D plasma electron/ion density and energy maps

Mishra, B., *et al.*, Front. in Physics, **10**, 932448, (2022)
Galatà, A., *et al.*, Front. in Physics, **10**, 947194, (2022)

RESULTS – Study of metal evaporation dynamics in ECRIS

Pidatella, A. *et al.,* Plasma Phys. Control. Fusion **66** (3), 035016 (2024)

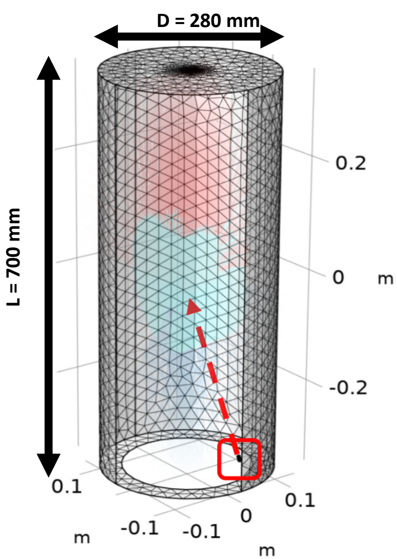

Oven: non-axisymmetric and tilted towards chamber center

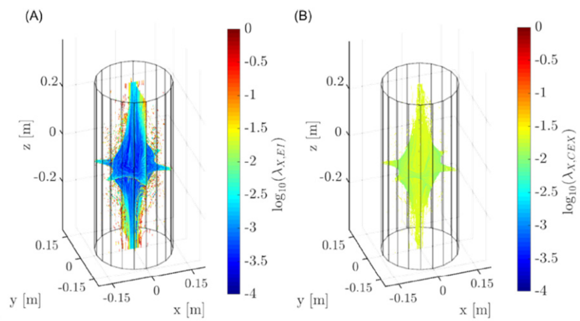

EI/CEX mean-free path

$$\lambda_{X,CEX} = \frac{v_X}{\sum_{i=1}^{Z} n_i \sigma_{CEX} \sqrt{v_X^2 + v_i^2}}$$

$$\lambda_{X,EI} = \frac{v_X}{n_e \sigma_{e,ion} \sqrt{v_X^2 + v_e^2}}$$

Cross-section for electron impact (EI) and charge-exchange (CEX) ionisation only 0⁺->1⁺

$$\sigma_{e,ion} = aq\frac{\ln E/I}{EI}$$

Lotz, W., Zeitschrift fur Physik 216, pp. 241–247, (1968).

$$\sigma_{CEX} = Ai^{\alpha} I^{\beta}$$

Müller, A. *et al.*, Phys. Lett. A, 62A:391-4, (1977).

NO PLASMA

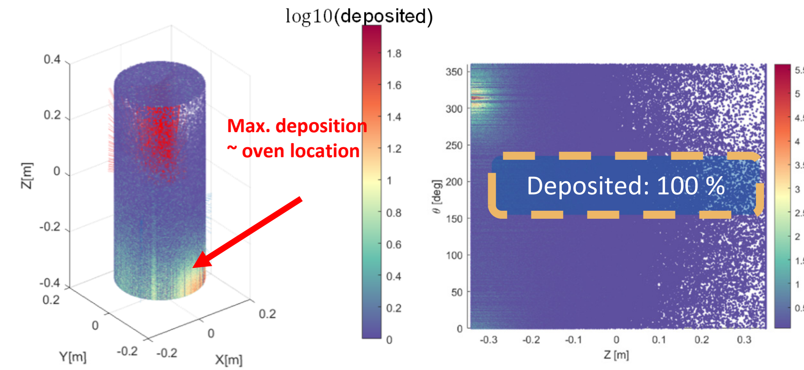

WITH PLASMA

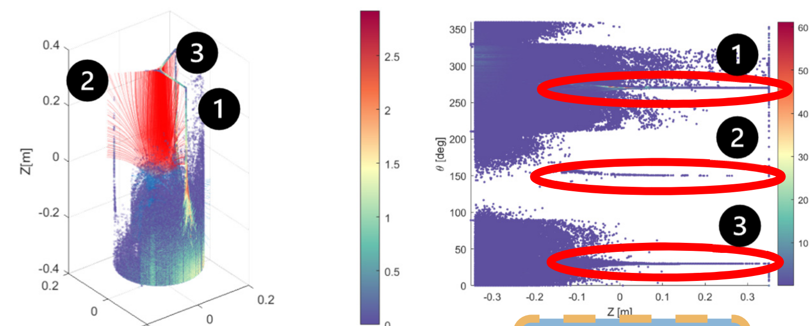

Deposited: 78 %
Reacting: 47 %

Simulation features:

- N. particles: 10^6, T_{sim} = 3e-3 s, δt = 1e-8 s

RESULTS – Study of metal evaporation dynamics in ECRIS

Pidatella, A. *et al.,* Plasma Phys. Control. Fusion **66** (3), 035016 (2024)

^{134}Cs diffusion & transport– no hot screen

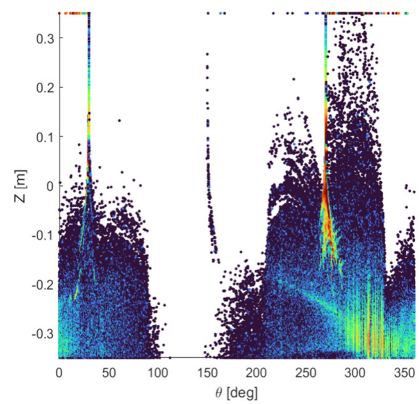

^{134}Cs – diffusion & transport with **hot screen (870 K)**

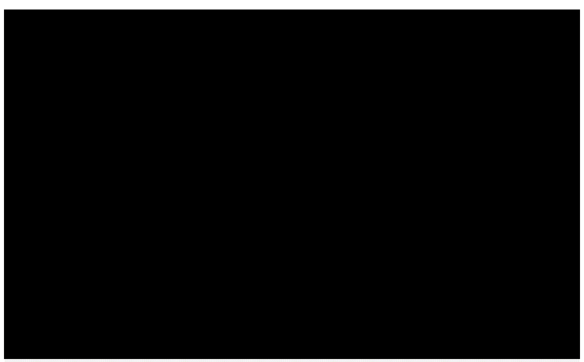

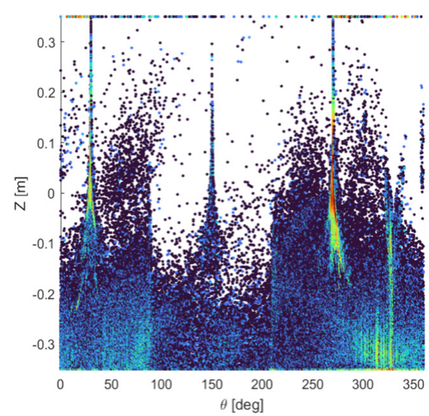

N° Ionisations 10^2 higher than no-liner

MAIN RESULT: γ signal arising from deposited short lived β-decaying Cs isotopes at the trap's wall is negligible along the detection sight-lines

APPLICABILITY and IMPACT

- Study for unconventional emitting surface of ovens: increasing exposure to the plasma
- Study for unconventional oven position: better coupled to the inner plasma region to improve efficiency
- Study evaporation strategies to reduce metal deposition or recycling of deposited: reduction of **long-term instabilities**
- Regions more exposed to metal fluxes for sensoring and online monitoring: QMC, OES, etc. – better assessment of sensor position

APPLICATION - How do ECR plasmas affect β-decay rates?

Mishra, B, Pidatella, A. *et al.*, arXiv:2407.01787 , https://doi.org/10.48550/arXiv.2407.01787

WHY?

- Novel approach complementary to Storage Rings experiments
- Investigating, for the first time, the **β-decaying nuclei half-life changes** using **magnetized laboratory plasma**

F. Bosch *et al*, Phys. Rev. Lett. **77**, 26 (1996)
M. Jung, F. Bosch *et al*, Phys. Rev. Lett. **69**, 2164 (1992)

In-plasma decay energy – Takahashi, Yokoi model

K. Takahashi and K. Yokoi, Nucl. Phys. A **404** (1983)
Mishra, B. *et al*. Frontiers in Phys. 10.3389/fphy.2022.932448 (2022)

$$Q = Q_0 + [E^*_X - E^*_Y] + [B_X - B_Y] - [B^*_{Xi} - B^*_{Yi'}] + [e^*_{X_{i,j}} - e^*_{Y_{i',j'}}] + \sum_{x=i}^{Z_X-1} \Delta_x - \sum_{x=i'}^{Z_Y-1} \Delta_x$$

Δ Nuclear energy levels

Δ Ionisation energy

Δ Excitation energy

Ionisation potential depression

In-plasma decay rate

$$\boxed{\lambda^*} = \ln 2 \sum_m \sum_{ij} p_{ij} \frac{f^*_m(ij)}{f_{m0} T_{1/2}}$$

Transition type

Atomic configuration (CSD of plasma)

LPV depends on transition m and ionisation - excitation level of atom.

Decay rate and *ft* values

$$\boxed{f_L(Z', Q_0)}\boxed{T_{1/2}} = \frac{(\ln 2) 2\pi^3 \hbar^7}{g^2 m_e^5 c^4 |\mathcal{M}^L_{if}|^2}$$

Lepton-phase volume (**LPV**) for **orbital EC/Bound-State Beta Decay**

$$f^*_m(ij) = \sum_{x(ij)} \sigma_x(\pi/2)[g_x \text{ or } f_x]^2 (Q/m_e c^2)^2 S_{(m)x(ij)}$$

- **New decay channels** can open, changing the decay rate
- Both *leptonic* (plasma-configuration) and *hadronic* (nuclear excitation) contributions matter in plasma decay rate change
- Plasma **charge state (CS)** and **level population (LP) distribution** of radionuclides drive the in-plasma decay

RESULT: How do ECR plasmas affect β-decay rates?

Mishra, B, Pidatella, A. *et al.*, arXiv:2407.01787 , https://doi.org/10.48550/arXiv.2407.01787

HOW?

PIC simulations of reacting ^{7}***Be ions in ECR plasma***:

- Description: Steady-state maps of plasma electrons and ions +Balance equation (EI + CEX) + ***W.I.P.*** : atomic excitations (electron collisional (de)excitation)
- Self-consistency: Electron/ion density and energy maps
- Scaling: Fraction of buffer ion density

PIC-MC simulated 3D ^{7}Be CSD 1 and 2 E.C. half-life in ECR plasma

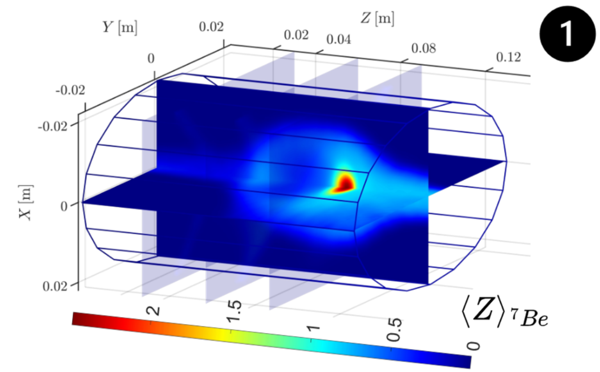

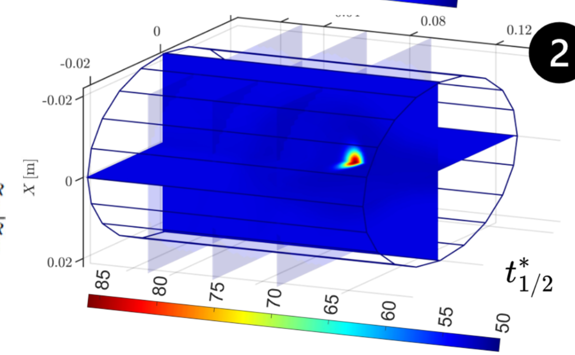

MODEL GENERATES 3D E.C. DECAY RATES IN ECR PLASMA!

3 core modules

Ion Transport

Transport in EM fields under Lorentz force

Poisson solver for ES field due to local charge unbalance

Collisions by Fokker-Planck equation

MC Sampling

$$\frac{dn_i^R}{dt} = \left[n_{i-1}^R n_e \gamma_{i-1,i} - n_i^R n_e \gamma_{i,i+1}\right] + \left[n_{i+1}^R \sum_{j=0}^{N-1} n_j E_{i+1,i} + n_{i-1}^R \sum_{j=1}^{N} n_j E_{i-1,i}\right] - \left[n_i^R \sum_{j=0}^{N-1} n_j E_{i,i-1} + n_i^R \sum_{j=1}^{N} n_j E_{i,i+1}\right] - \frac{n_i^R}{\tau_i^R}$$

Electron impact ionization (EI)

Ion impact charge exchange (CEX)

Density Scaling

Scaling of ^{7}Be ion density on plasma buffer ion occupation map

$$K \oint_V \sum_{i=0}^{4} k_i N_i^R dV = 0.01 \oint_V \sum_{i'=1}^{8} n_{i'} dV$$

RESULT: How do ECR plasmas affect β-decay rates?

Mishra, B, Pidatella, A. *et al.*, arXiv:2407.01787 , https://doi.org/10.48550/arXiv.2407.01787

Impact of *different isotope injection conditions* and *atomic excitation*

^{7}Be– starting normal distribution

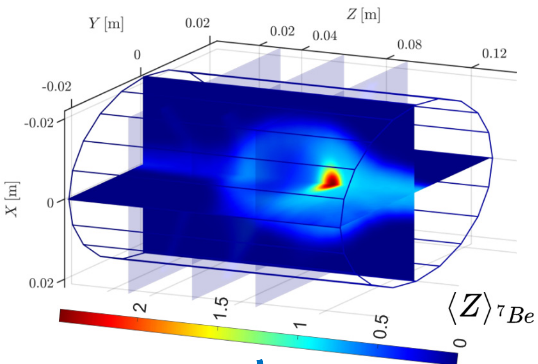

^{7}Be– starting injection of beam

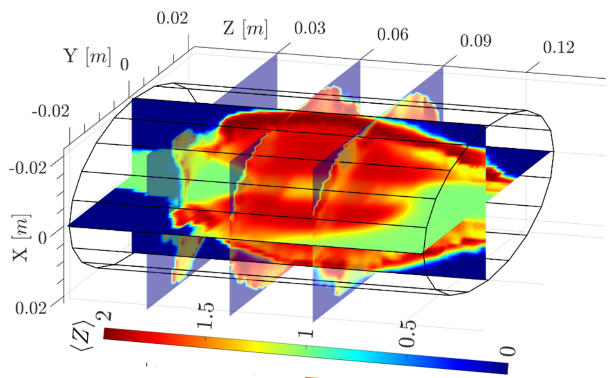

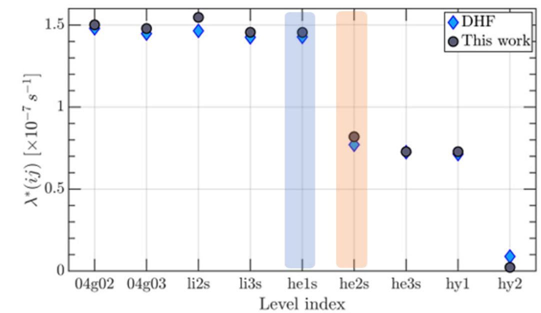

Figure 5: ^{7}Be configuration-dependent $\lambda^*(ij)$ calculated using our model and DHF [31, 41, 57].

^{7}Be– in-plasma half-life only GS

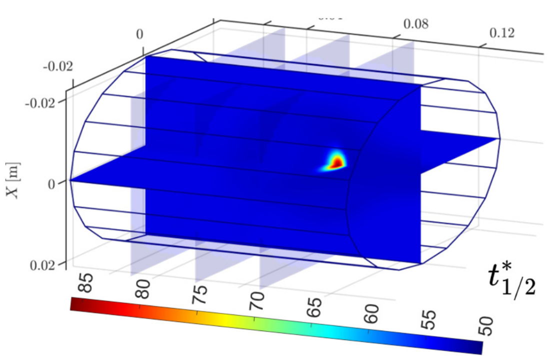

^{7}Be– in-plasma half-life only GS (up 2$^+$)

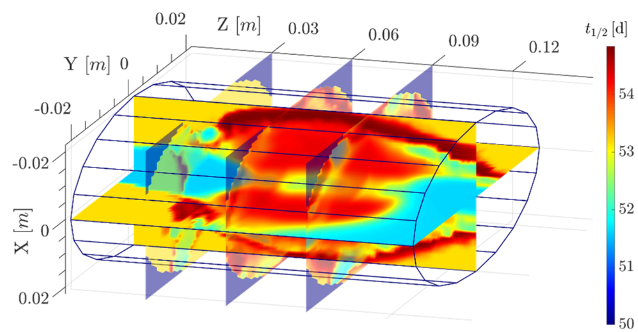

^{7}Be– in-plasma half-life with 1st ES (up 2$^+$)

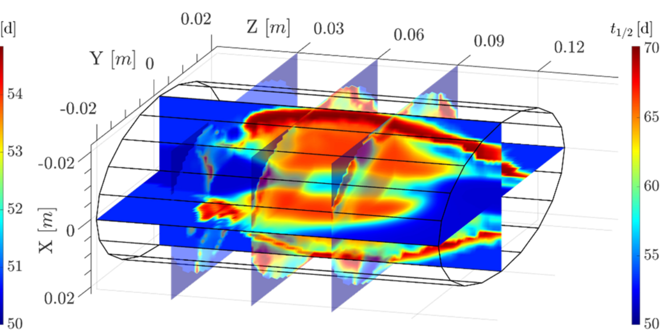

What’s next? – Outlook and perspectives

Salvia, C. *et al.*, Il Nuovo Cimento C **47** (271), (2024)

- **Wave propagation** and interaction in the plasma chamber by modelling a ***hot EM tensor***
- **1D semi-analytical model** studying EM propagation of fast wave X considering **ion cyclotron heating** in plasma
- Divertor Tokamak Test (DTT) plasma fusion scenario and profiles (electron/ion density, temperature, magnetic field)
- Linearised Vlasov Eqs. assuming plasma stationarity, homogeinity, no collisions, no strong EM perturbation solving for **collisionless EM wave damping in plasma** (e.g., Landau damping)

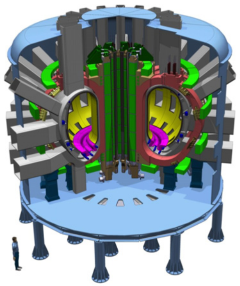

DTT scheme e 3-strap antenna design (60 Mhz) for ICRH

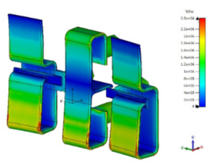

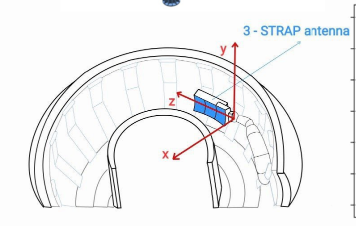

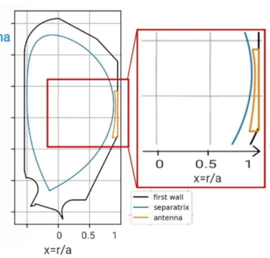

$$\vec{k} \wedge \vec{k} \wedge \tilde{\vec{E}}_{\vec{k},\omega} + \frac{\omega^2}{c^2} \underline{\underline{\varepsilon}}\left(\vec{k},\omega\right) \cdot \tilde{\vec{E}}_{\vec{k},\omega} = 0 \qquad \lambda_\alpha = \frac{k_x^2 v_{th\alpha}^2}{2\Omega_{c\alpha}^2}$$

$$\varepsilon_{ij} = \delta_{ij} - \sum_\alpha \Pi_{ij}^\alpha \sum_{n=-\infty} \Gamma_{ij}^n\left(\lambda_\alpha\right) Z_{ij}\left(x_{n\alpha}\right)$$

Plasma dispersion functions

Modified Bessel functions

$$-\frac{\partial^2 \tilde{E}_y}{\partial x^2} + \left[k_z^2 - \frac{\omega^2}{c^2}\left(\varepsilon_{yy}^H + i\varepsilon_{yy}^A\right) + \frac{\omega^4}{c^4} \frac{\left(\varepsilon_{xy}^H + i\varepsilon_{xy}^A\right)^2}{\left(k_z^2 - \frac{\omega^2}{c^2}\left(\varepsilon_{xx}^H + i\varepsilon_{xx}^A\right)\right)}\right] \tilde{E}_y = 0$$

Anti-hermitian term only accounts for EM wave damping

$$\epsilon_{yy}^A \approx \pi^{1/2} \left[\frac{k_x^2}{k_z^2} \frac{\omega_{pe}^2}{\Omega_{ce}^2} \frac{1}{x_{0e}} e^{-x_{0e}^2} + \frac{1}{2} \frac{\omega_{pD}^2}{\omega^2} x_{0D} e^{-x_{1D}^2} + \frac{1}{2} \frac{\omega_{pHe3}^2}{\omega^2} x_{0He3} e^{-x_{1He3}^2} \right]$$

Electron/Ion damping term at the fundamental harmonic resonance

$$\chi_{0e,0i} = \frac{\omega}{k_z v_{th,e/i}} \qquad \chi_{1i} = \frac{\omega - \Omega_{ci}}{k_z v_{th,i}}$$

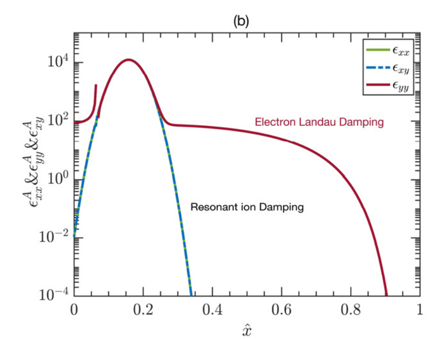

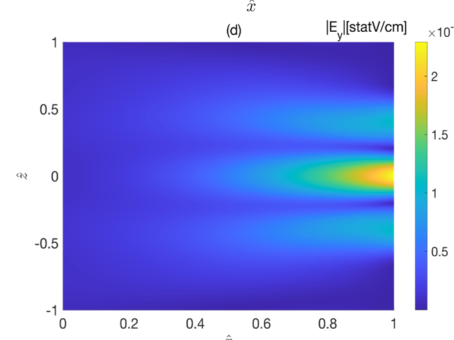

Summary and conclusions

- ECRIS useful for generating ion beams with tunable magnitude and charge states, but their internal plasma structure is complex
- **Full-wave PIC codes** which evolve density with EM field distribution **can furnish space-resolved maps of electron density and energy**
- The algorithm **could now be updated** to shift from **cold to hot electron tensor** description
- **PIC-MC codes**: **ion balance** equation self-consistently with electron charge distribution can furnish **space-resolved maps of CSD and excitation levels**
- Together these maps are powerful **predictive tools** to study **numerous ECR plasma phenomena** like **X-ray emission**, heavy element **opacity**, neutral **particle dynamics** and in-plasma **nuclear reactions**
- These simulations can **improve fundamental understanding of the operation of ECR ion sources** (instabilities, current generation) as well as for applications involving them (PANDORA facility)

Thanks for your attention!!

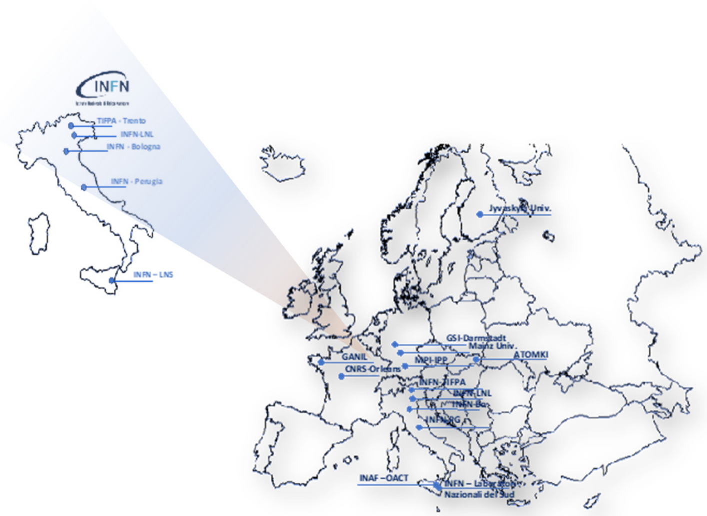

Also collaborating in the nuclear fusion research programme for the Divertor Tokamak Test (DTT) project